ISSN 2616-5767 Vol.7, Issue 2: 113-122, DOI: 10.25236/AJETS.2024.070217

Research on the Occurrence Law and Main Controlling Factors of Gas in the V_{9-10} Coal Seam of Pingdingshan Coal Mine No. 6

Sun Jiarui[1,2,a,*]

[1]*School of Energy Science and Engineering, Henan Polytechnic University, Jiaozuo, China*
[2]*Pingdingshan Coal Mine No. 6, Pingdingshan, China*
[a]*13837508312@163.com*
[*]*Corresponding author*

Abstract: *To study the occurrence of coal seam gas, the V_{9-10} coal seam of Pingdingshan Coal Mine No.6 was taken as the research object. Through field measurement, theoretical analysis and other methods, the occurrence law and main control factors of coal seam gas were comprehensively studied. According to the analysis of the gas emission and gas content during the production period of the mining face, geological structure, burial depth, and thickness of coal seam all affect the occurrence of coal seam gas. A comprehensive analysis was conducted on the influence of various geological factors on the gas occurrence in the V_{9-10} coal seam of Pingdingshan Coal Mine No.6. The results showed that geological structure and burial depth are the main factors affecting the deep gas occurrence in the V_{9-10} coal seam of Pingdingshan Coal Mine No.6.*

Keywords: *The Law of Gas Occurrence; Gas Geology; Geological Structure; Coal Seam Gas*

1. Introduction

In 2023, China's raw coal production reached 4.71 billion tons, with coal consumption accounting for 55.3% of the total energy consumption. Coal remains the main energy source in China[1]. With the increasing depth of coal mining and the increasingly complex geological conditions, many mines have entered deep areas of coal and gas outburst for mining, making gas control increasingly difficult[2]. Therefore, exploring the distribution and storage status of gas is of great significance for ensuring the safe mining of coal mines[3].

Gas is a gas geological body associated with coal seams. Studying the occurrence and migration laws of coal seam gas and revealing the geological laws of mine gas have important guiding significance for coal mine gas control work [4]. A large number of scholars at home and abroad have conducted extensive research on the occurrence laws of coal seam gas from the aspects of geological structure and coal seam occurrence characteristics, and have achieved significant results. Some scholars have studied the control effect of geological structures on gas occurrence through the construction of hierarchical control theory [5,6]. Some scholars have also studied the direct impact of different types of structures on gas occurrence [7,8,9,10]. Scholars have also studied the control effect of gas occurrence from aspects such as coal seam burial depth, overlying bedrock thickness, and coal seam thickness [11,12,13].

The V_{9-10} coal seam of Pingdingshan Coal Mine No.6 is the main mining coal seam of the mine. This article takes this coal seam as the research object and comprehensively analyzes the gas occurrence law and main control factors of the V_{9-10} coal seam through on-site measurement, theoretical analysis, and other methods, providing a theoretical basis for mine gas control work.

2. Characteristics of Gas Storage in the V_{9-10} Coal Seam

The occurrence of coal seam gas is constrained by geological factors such as burial depth, structure, and the rock properties of the coal seam roof and floor. For different mining areas, the impact of various geological factors on gas content varies. Among many geological factors, there is always one or two dominant factors that control the overall trend of gas content changes throughout the entire mining area. Other factors can only affect the occurrence of coal seam gas locally. The gas parameters of the V_{9-10} coal seam in Pingdingshan Coal Mine No.6 are shown in Table 1.

ISSN 2616-5767 Vol.7, Issue 2: 113-122, DOI: 10.25236/AJETS.2024.070217

Table 1: Gas Pressure and Content of Coal Seams from $V_{9\text{-}10}$.

Measurement location	Gas pressure (MPa)	Gas content (m^3/t)	Elevation (m)	Burial depth (m)
V_8—22160 transportation roadway 1000m inward	0.52		-575	795
V_8—22160 transportation roadway 940m inward	0.22		-574	794
V_8—22160 transportation roadway 520m inward	0.2		-567	787
The opening of the three level east dedicated return airway is 300m downwards	0.3	3.70	-649	839
The opening of the three level east dedicated return airway is 400m downwards	0.1		-667	847
The opening of the three level east dedicated return airway is 580m downwards	0.9	3.78	-689	869
The opening of the three level east dedicated return airway is 750m downwards	1.3		-700	890
The opening of the three level east dedicated return airway is 770m downwards	0.25	4.18	-702	892
V_8—22310 transportation roadway 100m inward	0.2		-727	912
V_8—22310 transportation roadway 120m inward	0.75	2.99	-738	918
V_8—22310 transportation roadway 450m inward	1.33	4.47	-727	912
V_8-22220 concentrated return air alley 160m inward	0.26	3.3580	-691	890
V_8-22220 concentrated return air alley 570m inward	0.79	3.6510	-696	904
V_8-22220 concentrated return air alley 970m inward	0.21	3.8906	-694	908
V_8-22220 concentrated return air alley 1370m inward	0.81	3.4711	-698	896
V_8-22220 mining car yard of transportation roadway point vehicle 8	0.47	3.2600	-665	880
V_8-22220 open-off cut and High pumping alley Point 2 is 20 m inward	0.03	3.5709	-691	886
V_8-22220 open-off cut and High pumping alley Point 2 is 25 m inward	0.23	3.5690	-687	882
V_8-22220 open-off cut and High pumping alley Point 5 is 16.5 m outward	0.20	3.4144	-665	870
V_8-22220 mining car yard of return airway point vehicle 2	0.58	4.1435	-708	892
V_8-32020 mining car yard of return airway point L4’	0.25	3.6094	-768	914
V_8-32020 mining car yard of transportation roadway Point +1 is 33 m outward	0.20	3.5446	-795	946
V_8-32020 transportation roadway Point +3 is 15 m outward	0.65	3.7759	-797	953
V_8-32020 transportation roadway Point +9 is 69 m outward	0.20	3.6251	-800	967
V_8-32020 transportation roadway Point +11 is 24 m outward	0.77	4.2974	-808	970
V_8-32020 transportation roadway Point +16 is 73 m outward	0.89	3.1246	-812	972
V_8-32020 transportation roadway Point +21 is 46 m outward	0.60	4.2995	-827	985
V_8-32020 transportation roadway Point +24 is 46 m inward	0.60	3.9474	-845	995
V_8-32020 transportation roadway and open-off cut turning point	0.55	4.0141	-863	1003
V_8-32020 from the turning point of the transportation lane and cutting eye is 50m inward	0.58	4.0942	-829	989

2.1 Reverse calculation of gas content based on gas emission volume

The scope of the Pingdingshan Coal Mine No.6 fields is relatively large, making it difficult to fully

ISSN 2616-5767 Vol.7, Issue 2: 113-122, DOI: 10.25236/AJETS.2024.070217

indicate the distribution of gas content in the entire area. Therefore, in order to explore the distribution characteristics of gas content in the mined areas, the absolute gas emission data of the $V_{9\text{-}10}$ coal seam mining face is used to calculate the corresponding gas content as a supplement to the data. According to the actual production layout, three working faces are selected on the east and west wings of the second mining area of the V coal seam, and the calculation formula is as follows[14]:

$$W = \frac{1440\bar{Q}}{(1-C)q}K + R \tag{1}$$

In the formula: W—Gas content of raw coal, m^3/t; K—Gas emission composition parameters, Based on the actual production situation of the mining face, K takes the ratio of the gas emission in the first month to the second month, and the statistics are summarized in Table 2; Q—Monthly absolute gas emission, m^3/min; q—Daily average production, t; R—Residual gas content, m^3/t； C—Deduction coefficient(C=30/A, A is the mining length of the mining face, m).

Table 2: Composition parameter K of gas emission from mining face

Mining face	22160	22180	22310	22290	22200	22290-
Composition parameter K of gas emission amount	0.418	0.910	0.912	0.952	0.657	0.625

The residual gas content is determined from Table 3 based on the actual mining situation of the coal seam and the volatile matter yield of the coal[15]. The average volatile matter yield of the $V_{9\text{-}10}$ coal seam is 34.59%, and its residual gas content is taken as 2 m^3/t.

Table 3: Table of residual gas content values of coal

Volatile fraction yield of coal, Vdaf(%)	12~18	18~26	26~35	35~42	42~50
Residual gas content in coal, R(m^3/t)	4~3	3~2	2	2	2

The average calculated gas content of the $V_{9\text{-}10}$-22200 mining face was 3.654 m^3/t, while the actual value was 3.651 m^3/t. It was found that the predicted results were close to the measured results. The gas content of the $V_{9\text{-}10}$ coal seam was calculated using the absolute gas emission data during the mining period, and the gas content value of the mining face was obtained. The results are shown in Table 4.

Table 4: Results of Back Calculation of Gas Content in the $V_{9\text{-}10}$ coal seam of Pingdingshan Coal Mine No.6

Mining face	Absolute gas emission (m^3/min)	Gas content(m^3/t)	Mining face	Absolute gas emission (m^3/min)	Gas content(m^3/t)
$V_{9\text{-}10}$-22160	1.60	2.30	$V_{9\text{-}10}$-22290-	1.80	3.44
	3.83	2.72		2.88	4.31
	3.68	2.69		2.35	3.88
	3.40	2.64		2.25	3.80
	3.96	2.74		1.20	2.96
	3.51	2.66	$V_{9\text{-}10}$-22310	7.00	4.99
	3.60	2.68		5.94	4.54
	3.50	2.66		4.68	4.00
	3.60	2.68		5.13	4.19
$V_{9\text{-}10}$-22180	2.82	3.91		5.95	4.54
	3.10	4.10		3.80	3.62
	2.71	3.84		7.00	4.99
	3.20	4.17		3.98	3.70
	3.05	4.07		3.35	3.43
	3.63	4.46		3.85	3.65
	3.03	4.05		3.55	3.52
	3.15	4.13		3.69	3.58
	3.24	4.19		3.18	3.36
	2.95	4.00		4.63	3.98
	3.28	4.22		3.39	3.45
	3.36	4.28		4.88	4.09
	3.32	4.25		3.57	3.53

ISSN 2616-5767 Vol.7, Issue 2: 113-122, DOI: 10.25236/AJETS.2024.070217

Mining face	Absolute gas emission (m^3/min)	Gas content(m^3/t)	Mining face	Absolute gas emission (m^3/min)	Gas content(m^3/t)
	3.55	4.40		4.61	4.90
	3.34	4.26		4.84	5.04
	3.15	4.13		4.74	4.98
	3.42	4.32	V_{9-10}-22290	4.51	4.84
	3.33	4.26		4.88	5.07
	3.21	4.17		4.39	4.76
V_{9-10}-22200	2.52	3.02		4.42	4.78
	4.20	3.69		4.64	4.92
	3.53	3.42		4.72	4.97
	3.72	3.50		4.30	4.70
	3.92	3.58		4.10	4.58
	4.25	3.71		4.30	4.70
	4.40	3.77		2.80	3.76
	3.70	3.49		1.70	3.07
V_{9-10}-22200	2.29	2.92		1.60	3.01
	4.66	3.88		1.58	2.99
	4.07	3.64		1.55	2.97
	2.36	2.95		4.18	4.63
	3.75	3.51	V_{9-10}-22290	4.18	4.63
	1.95	2.79		4.09	4.57
	2.62	3.06		4.29	4.70
	2.67	3.08		3.22	4.02
	3.90	3.57		3.13	3.97
	4.60	3.85		2.42	3.52
V_{9-10}-22200	4.60	3.85		2.12	3.33
	4.70	3.89		2.12	3.33
	3.29	3.33		2.15	3.35
	3.90	5.13		2.22	3.40
	3.08	4.47		2.06	3.30
V_{9-10}-22290-	2.88	4.31		2.00	3.26
	1.98	3.59			

2.2 Gas pressure characteristics of V_{9-10} coal seam

As shown in Table 1, a total of 30 gas pressure points were measured in the measurement area of -567~-863 m. The measured gas pressure was 0.03~1.33 MPa, with an average value of 0.45 MPa. Regression fitting of gas pressure in V_{9-10} coal seam is shown in Figure 1, and the linear equation is:

$$P = 0.0016H - 0.9267 \quad (2)$$

In the formula: P—Coal seam gas pressure, MPa; H—Coal seam occurrence depth, m.

From the fitting relationship between gas pressure and coal seam burial depth, it can be seen that the gas pressure in the V_{9-10} coal seam of Pingdingshan Coal Mine No.6 shows a roughly linear increasing relationship with the increase of burial depth. The measured maximum pressure of the V_{9-10} coal seam is 1.33 MPa, with an elevation of -727 m and a burial depth of 912 m. The gradient of gas pressure growth in the coal seam is 0.16 MPa/100 m.

ISSN 2616-5767 Vol.7, Issue 2: 113-122, DOI: 10.25236/AJETS.2024.070217

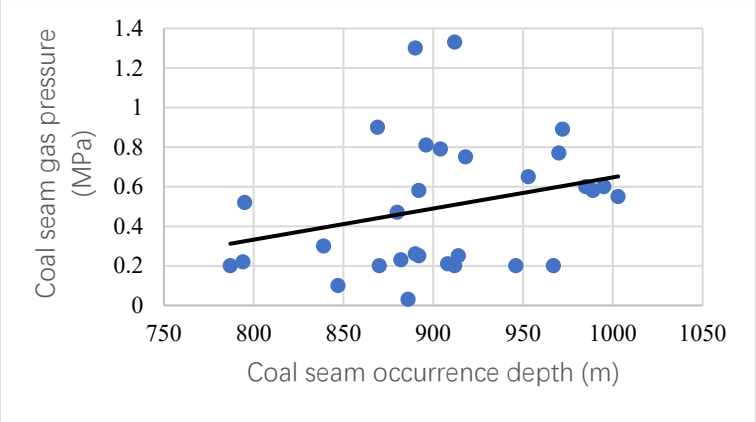

Figure 1: Gas pressure variation with burial depth in the $V_{9\text{-}10}$ coal seam of Pingdingshan Coal Mine No.6.

2.3 Gas content characteristics of $V_{9\text{-}10}$ coal seam

According to Table 1, a total of 32 gas content points were measured at the coal seam floor elevation of -567~-863 m, with a gas content of 2.99~4.47 m^3/t and an average of 3.64 m^3/t. Regression fitting of gas content in $V_{9\text{-}10}$ coal seam is shown in Figure 2, and the linear equation is:

$$W = 0.0025H + 1.4357 \quad (3)$$

In the formula: W—Coal seam gas content, m3/t; H—Coal seam occurrence depth, m.

From the fitting relationship between gas content and coal seam burial depth, it can be seen that the gas content in the $V_{9\text{-}10}$ coal seam of Pingdingshan Coal Mine No.6 shows a roughly linear increasing relationship with the increase of burial depth. The maximum measured content of coal seam $V_{9\text{-}10}$ is 4.47 m^3/t, with an elevation of -727 m and a burial depth of 912 m. The gradient of gas content growth in the coal seam is 0.25 $m^3/t/100$ m.

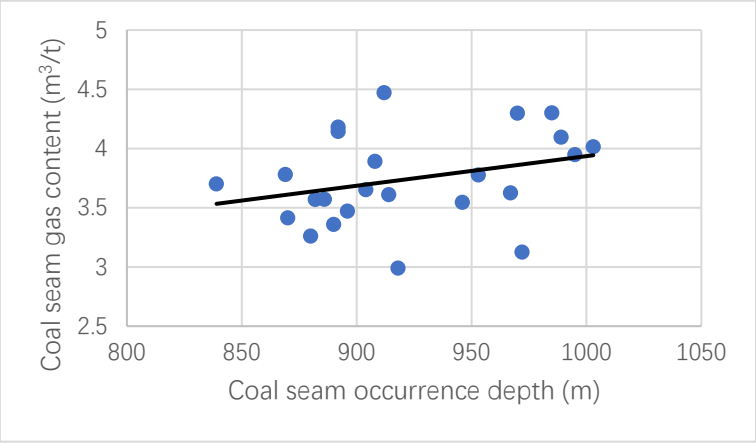

Figure 2: Gas content variation with burial depth in the $V_{9\text{-}10}$ coal seam of Pingdingshan Coal Mine No.6.

According to Table 2, it can be seen that among the three mining faces of $V_{9\text{-}10}$-22160, $V_{9\text{-}10}$-22180, and $V_{9\text{-}10}$-22200 in the western part of the second mining area of the V coal seam, the gas content in the $V_{9\text{-}10}$-22180 mining face is the highest, followed by the $V_{9\text{-}10}$-22200 mining face, and the gas content in the $V_{9\text{-}10}$-22160 mining face is the lowest. The spatial position relationship of the three mining faces is that they are arranged downwards in sequence: $V_{9\text{-}10}$-22160, $V_{9\text{-}10}$-22180, and $V_{9\text{-}10}$-22200. The burial depth of the $V_{9\text{-}10}$-22200 mining face is the highest, and the burial depth of the $V_{9\text{-}10}$-22160 mining face is the shallowest. Due to the fact that the $V_{9\text{-}10}$-22180 mining face was the first to be mined, only the goaf of the Wu8 coal seam was overlying, and all other directions were solid. Therefore, during the mining period, the gas emission was the largest, and the gas content was also relatively high when calculated. The gas concentration in the $V_{9\text{-}10}$-22200 mining face is higher than that in the $V_{9\text{-}10}$-22160 mining face, indicating a positive correlation between gas content and burial depth.

ISSN 2616-5767 Vol.7, Issue 2: 113-122, DOI: 10.25236/AJETS.2024.070217

Analyze the relationship between the spatial position and gas content of the three mining faces of V_{9-10}-22290, V_{9-10}-222310, and V_{9-10}-22310 in the eastern part of the second mining area of the V coal seam. The spatial position relationship of the three mining faces is that the mining faces of V_{9-10}-22290, V_{9-10}-22290, and V_{9-10}-22310 are arranged downwards in sequence. The mining face of V_{9-10}-22310 has the highest burial depth, while the mining face of V_{9-10}-2290 has the shallowest burial depth. Due to the gradual change in burial depth in this area, the gas content in the three mining faces is basically consistent, and there is no significant positive correlation between gas content and burial depth.

The contour map of the gas content in the working face was drawn based on the reverse calculation of the gas content. Taking the mining faces of V_{9-10}-22180 and V_{9-10}-22290 as examples, the influencing factors of gas occurrence in shallow mined areas were determined through the analysis of geological structure, coal seam thickness, and other data. The contour maps of gas content in the mining faces of V_{9-10}-22180 and V_{9-10}-22290 are shown in Figures 3 and 5.

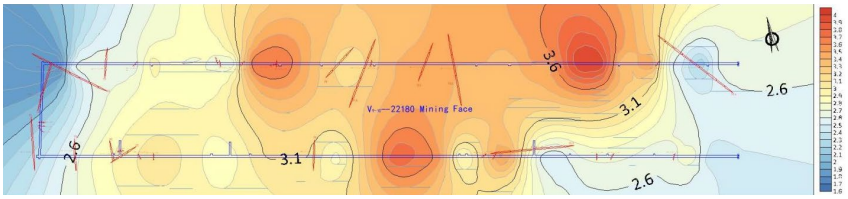

Figure 3: Contour map of gas content in the mining face of V_{9-10}-22180.

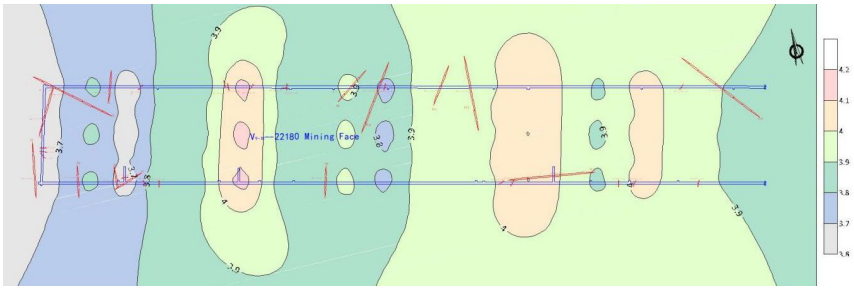

Figure 4: Contour map of coal thickness in V_{9-10}-22180 mining face.

By comparing the contour maps of gas content and coal thickness in the V_{9-10}-22180 mining face (Figure 4), the influencing factors of gas occurrence are analyzed. A total of three faults with a drop greater than 1 m and three small faults were exposed near the V_{9-10}-22180 open-off cut. Therefore, the gas near the open-off cut escaped along the structural fractures, resulting in a lower content. At 835 m inward from the opening of the transportation lane, the F10 fault is exposed, and gas escapes along the structural cracks, resulting in a decrease in content. The coal thickness gradually thickens from the cutting hole outward, and the gas also gradually increases.

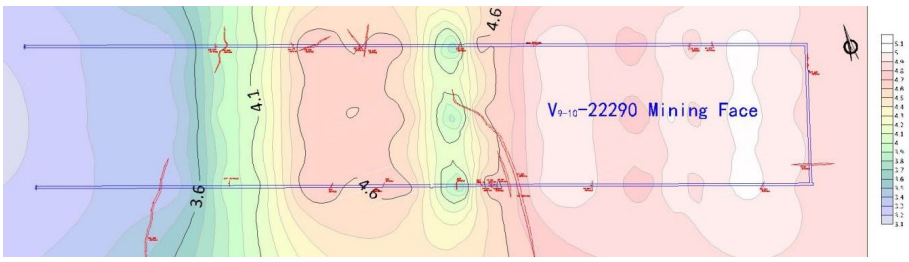

Figure 5: Contour map of gas content in the mining face of V_{9-10}-22290.

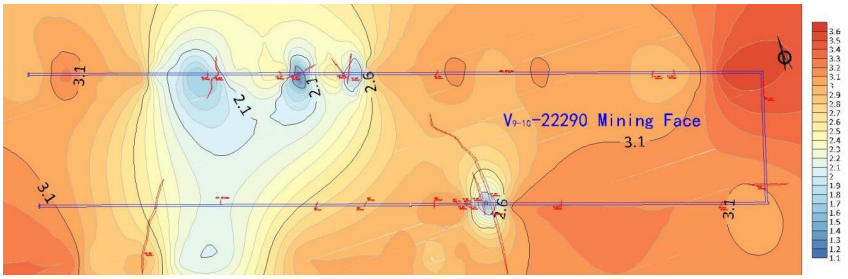

Figure 6: Contour map of coal thickness in V_{9-10}-22290 mining face.

ISSN 2616-5767 Vol.7, Issue 2: 113-122, DOI: 10.25236/AJETS.2024.070217

By comparing the contour maps of gas content and coal thickness in the V_{9-10}-22290 mining face (Figure 6), the influencing factors of gas occurrence are analyzed. A total of three faults with a drop greater than 5 m were exposed in the return air roadway from V_{9-10}-22290, namely F21 fault at 265 m inward from the opening of the return air roadway, F8 fault at 1013 m, and F7 fault at 1032 m. Affected by the F8 and F7 faults, gas escapes through structural fractures, resulting in a lower gas content at 850 m inward from the opening of the return airway. As shown in Figure 6, there are some areas outside the mining face where the coal thickness is less than 2 m, and there is an F21 fault as a gas escape channel. Therefore, the gas content within the 570 m range outside the mining face is relatively low.

Based on the field measurement gas content and the gas content calculated based on the gas emission from the mining face, compare the gas content on the eastern and western part of the second mining area of the V coal seam. The average measured gas content in the west wing of the second mining area of the V coal seam is 3.61 m3/t, and the average value in the eastern part is 3.82 m3/t; The gas content calculated by reverse calculation of gas emission from the mining face has an average value of 3.58 m3/t in the western part mining area and 4.06 m3/t in the eastern part mining area. This can verify the accuracy of the prediction of gas content in the region based on gas pressure in the previous text.

3. Analysis of controlling factors for gas occurrence in the V_{9-10} coal seam

3.1 The control of geological structure on gas occurrence

The Pingdingshan Coal Mine No.6 is located in the southwest wing of the Likou syncline, which is a gently inclined monoclinic structure. There is no intrusion of magmatic rocks within the mining area. The direction of the strata is 125 ° in the middle of the mine, gradually turning north to 105 °, and approximately 85-100 ° in the east and west of the mine; The stratigraphic dip is mainly 0-30 °. The dip angle of the stratum is generally 10-15 °, and the depth is relatively gentle, ranging from 6-8 °; Near the southwest boundary, due to geological folds, there are significant changes in dip angles. The complexity of geological structures in the Pingdingshan Coal Mine No.6 is evaluated as moderate, and the gas in the V_{9-10} coal seam is mainly controlled by two aspects of geological structures: fold structures and fault structures.

There are no large fold structures developed within the scope of the Pingdingshan Coal Mine No.6, only three secondary associated folds. The shallow part has Shanzhuang syncline, while the deep part has Wanglou anticline and Naodian syncline. The Wanglou anticline is connected to the Naodian syncline, forming a continuous fold. The dip angle of the rock layers on both wings is relatively gentle, which basically controls the development of deep coal seams. Due to the deep fold structure being a wide and gentle associated fold with a large burial depth, it will not cause large-scale gas escape, only a small amount of gas migration will exist.

Due to the influence of regional structures, the small faults developed within the mining area of the Pingdingshan Coal Mine No.6 are mainly high angle normal faults, with the main strike directions being northeast and northeast, followed by nearly north-south directions. The dip angle of the faults is generally around 70 º, and the drop is basically less than 2 m. According to the actual production situation, the small fault itself does not store gas, but provides a channel for gas migration. Therefore, when mining activities progress near the fault, the amount of gas emission increases. According to three-dimensional geological exploration, there are DF105 and DF108 normal faults in the western part of the deep mining area, and DF120 normal fault in the central part, with a drop of more than 20 m, providing a good channel for gas escape. According to the gas geological laws of the shallow mined areas, the gas occurrence in the deep areas is also low in the west and high in the east.

3.2 The control of coal seam burial depth on gas occurrence

Draw the contour map of the burial depth of the V_{9-10} coal seam based on the data from exploration boreholes, as shown in Figure 7. The burial depth of the V_{9-10} coal seam gradually deepens northward, but due to the hilly terrain on the ground, the rate of burial depth deepening northward is not fixed. The southern part is mountainous, with a faster rate of burial depth deepening, while the northern part is plain, with a slower rate of deepening. Due to the influence of the Naodian syncline and Wanglou anticline, the rate of increase in burial depth in the west is greater than that in the east. Based on the previous analysis of the relationship between shallow gas content, pressure, and burial depth, it can be concluded that the gas occurrence in the Pingdingshan Coal Mine No.6 is generally positively correlated with burial depth.

ISSN 2616-5767 Vol.7, Issue 2: 113-122, DOI: 10.25236/AJETS.2024.070217

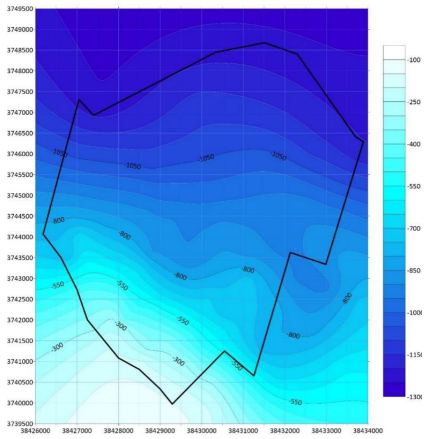

Figure 7: Contour map of the burial depth in the $V_{9\text{-}10}$ coal seam of Pingdingshan Coal Mine No.6.

3.3 The control of gas storage by surrounding rock properties

The $V_{9\text{-}10}$ coal seam and the V_8 coal seam belong to the V coal seam, and the interlayer spacing is small. Therefore, the rock layer between the $V_{9\text{-}10}$ coal seam and the V_8 coal seam is considered as the roof of the $V_{9\text{-}10}$ coal seam. The direct roof of $V_{9\text{-}10}$ coal seam in Liukuang is mainly composed of sandy mudstone and sandstone, and the main roof is sandy mudstone; The direct bottom plate is mudstone, and the old bottom is sandy mudstone. The rock properties of the top and bottom slabs of the $V_{9\text{-}10}$ coal seam are not conducive to gas emission and have a significant impact on the occurrence of coal seam gas. The lower part of the $V_{9\text{-}10}$ coal seam is the self formed coal seam, with a interlayer spacing greater than 70 m. Within the scope of the mine field, the influence of the bottom plate of the $V_{9\text{-}10}$ coal seam on gas occurrence is basically unchanged, so the rock layer of the bottom plate will not be discussed. Based on the data from exploration boreholes, a contour map of the spacing thickness between the $V_{9\text{-}10}$ coal seam and the V_8 coal seam was drawn, as shown in Figure 8.

The spacing between the $V_{9\text{-}10}$ coal seam and the V_8 coal seam varies greatly within the scope of the Pingdingshan Coal Mine No.6, with a thickness of 1-37 m. The distance between the $V_{9\text{-}10}$ coal seam in the west and the V_8 coal seam is generally greater than 10 m, while it is generally less than 10m in the east. According to geological data analysis, the Naodian syncline and Wanglou anticline are the reasons for this phenomenon. Synclines are generally formed by compression, and the rock layers in the axis are generally thickened, while the rock layers in the anticline axis are generally thinned due to tension. From this, it can be seen that geological structures also have an impact on the occurrence of deep gas in the Pingdingshan Coal Mine No.6 from other aspects. Within the scope of the Pingdingshan Coal Mine No.6, the roof lithology of the $V_{9\text{-}10}$ coal seam is basically the same, but the thickness changes significantly. Therefore, the influence factor of the surrounding rock properties on the gas occurrence of the $V_{9\text{-}10}$ coal seam is the roof thickness. Overall, areas with a thick roof have a larger gas accumulation.

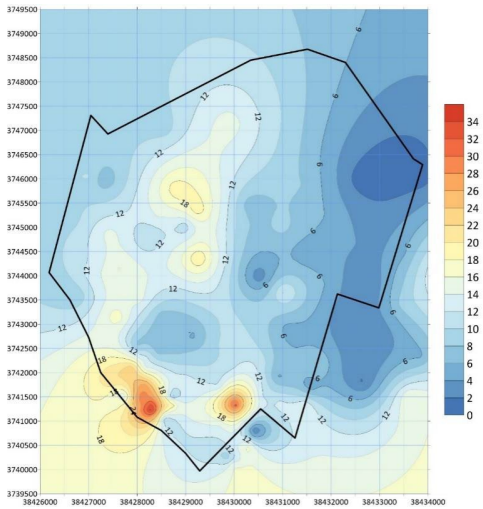

Figure 8: Contour map of the spacing between the $V_{9\text{-}10}$ coal seam and the V_8 coal seam in the Pingdingshan Coal Mine No.6.

ISSN 2616-5767 Vol.7, Issue 2: 113-122, DOI: 10.25236/AJETS.2024.070217

3.4 The control of coal seam thickness on gas occurrence

Draw the contour map of coal thickness in the $V_{9\text{-}10}$ coal seam based on the data from exploration boreholes, as shown in Figure 9. As shown in the contour map of coal thickness for the $V_{9\text{-}10}$ coal seam, the thickness of the $V_{9\text{-}10}$ coal seam is unstable and fluctuates greatly, ranging from 1.7 to 3.2 meters. The overall thickness of the deep coal seam in the Pingdingshan Coal Mine No.6 is thick in the west and thin in the east; The thickness of the coal seam in the southern part of the mining area is relatively thick, basically greater than 2.2 meters, but there are also some areas where the coal thickness is less than 1.7 meters. Similarly to the variation law of roof thickness, the variation of coal seam thickness is also influenced by the Naodian syncline and Wanglou anticline. Syncline is formed by compression, and soft rocks in the axis, such as coal seams, move towards the two wings due to the compression of hard rocks. Therefore, the syncline will cause the surrounding rock to thicken and the coal seams to become thinner. During the formation process of an anticline, the two wings are subjected to compressive stress while the axis is subjected to tensile stress, resulting in the anticline axis being a good storage space for minerals, thus thickening the coal seam. In summary, geological structure is the main factor leading to unstable changes in the thickness of deep coal seams in the Pingdingshan Coal Mine No.6. Therefore, coal seam thickness is also a factor affecting gas occurrence. Generally speaking, areas with larger coal seam thickness also have larger gas reserves.

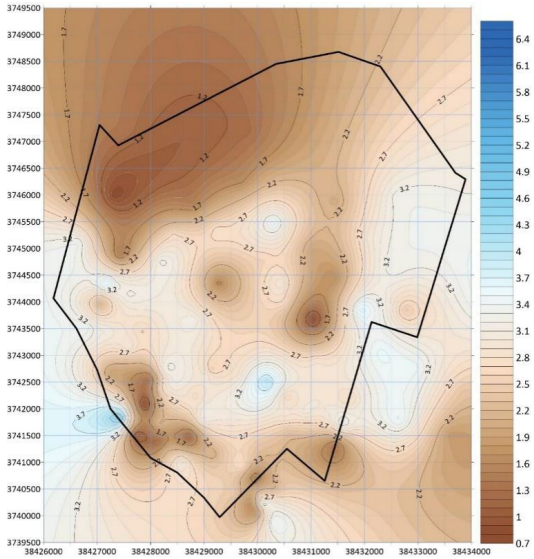

Figure 9: Contour map of coal thickness in the V9-10 coal seam of Pingdingshan Coal Mine No.6.

4. Conclusion

Through in-depth analysis of the occurrence law and main controlling factors of gas in the $V_{9\text{-}10}$ coal seam of Pingdingshan Coal Mine No.6, the following conclusions have been drawn:

(1) By conducting linear regression fitting on the measured gas pressure, content, and burial depth of the $V_{9\text{-}10}$ coal seam of Pingdingshan Coal Mine No.6, the results show a positive correlation between gas pressure, content, and burial depth. Comparing the gas pressure on the eastern and western part of the second mining area of the V coal seam of the Pingdingshan Coal Mine No.6, it was found that the gas pressure on the eastern part was higher than that on the western part. Based on the gas emission during the mining period of the mining face, calculate the gas content and select two mining faces from the eastern and western part of the second mining area of the V coal seam for analysis. From the entire mining area, the average coal thickness in the western part is thinner than that in the eastern part, so the overall gas content in the western part is lower than that in the eastern part. From a specific working face perspective, geological structure, burial depth, and coal seam thickness all affect the gas emission and gas content of the mining face.

(2) There are no large fold structures developed within the scope of the Pingdingshan Coal Mine No.6, and deep areas include Wanglou anticline and Naodian syncline. Due to the influence of regional structures, the small faults developed within the mining area of Pingdingshan Coal Mine No.6 are mainly high angle normal faults. There are multiple faults with a drop greater than 20 m developed in the deep

ISSN 2616-5767 Vol.7, Issue 2: 113-122, DOI: 10.25236/AJETS.2024.070217

mining area, providing a good channel for gas escape.

(3) The overall gas content in the V_{9-10} coal seam of Pingdingshan Coal Mine No.6 increases with the increase of coal seam burial depth. The amount of gas emission from the research area and surrounding mines is positively correlated with the burial depth of the coal seam. The burial depth of the V_{9-10} coal seam gradually deepens northward, and is affected by the Naodian syncline and Wanglou anticline. The rate of increase in burial depth in the west is greater than that in the east.

(4) Within the scope of the Pingdingshan Coal Mine No.6, the roof lithology of the V_{9-10} coal seam is basically the same, but the thickness changes significantly. Therefore, the influence factor of the surrounding rock properties on the gas occurrence of the V_{9-10} coal seam is the roof thickness. The thickness of coal seams is unstable and fluctuates greatly. Generally speaking, areas with larger coal seam thickness have higher gas content. The irregular phenomenon of roof thickness and coal seam thickness is caused by geological structures. Controlled by geological structures, the V_{9-10} coal seam in the western part of the Pingdingshan Coal Mine No.6 is relatively thin and the roof is thicker; The eastern coal seam is thicker and the roof is thinner.

References

[1] National Bureau of Statistics of the Communist Party of China. Statistical Bulletin on National Economic and Social Development of the People's Republic of China in 2023 [N]. People's Daily, 2024-3-1 (012).
[2] Zhang Zimin. Gas Geology [M]. Xuzhou: China University of Mining and Technology Press, 2009.
[3] Zhang Tiegang. Comprehensive treatment technology for mine gas [M]. Beijing: Coal Industry Press, 2001:267-301.
[4] Yuan Chongfu. Development and Application of Gas Geology in China [J]. Journal of Coal Science, 1997, 22 (6): 8-12.
[5] Zheng Lijun, Li Yanfei, Sun Wei, et al. Analysis of gas occurrence patterns based on gas geological unit division [J]. Coal Technology, 2023, 42 (08): 173-176.
[6] Tian Huanzhi, Jiang Mingquan, Yu Zhaoyang et al. Study on the geological structure characteristics of the Gemudi syncline and its impact on gas occurrence [J]. Coal Mine Safety, 2022, 53 (08): 149-154.
[7] Xiao Peng, Wu Mingchuan, Shuang Haiqing, et al. The occurrence pattern of coalbed methane under the influence of coal bearing normal fault zones [J]. Coalfield Geology and Exploration, 2022, 50 (10): 16-25.
[8] Zhou Yang, Shu Longyong, Liu Xue, et al. Study on the Stress and Gas Storage Law of Different Forms of Normal Fault Mining [J]. Coal Technology, 2023, 42 (06): 179-184.
[9] Sun Xiaoming, Zhao Jing, Lian Zhenshan. Study on the development characteristics of composite structures of collapse columns and faults and their impact on gas occurrence [J]. Coal Mine Safety, 2020, 51 (06): 14-18.
[10] Han Songlin, Zhao Yajuan, Gao Lin et al. Gas geological zoning and gas anomaly analysis: A case study of the No. 22 coal seam in Shunhe Coal Mine [J]. Coal Science and Technology, 2021, 49 (11): 150-156.
[11] Jiangyi H, Wulin L, Chao Z .Study on Geological Structure and Gas Content Occurrence Regularity of Gas Mine [J]. IOP Conference Series: Earth and Environmental Science, 2020, 455012006-012006.
[12] Deyang W, Yuanping C, Liang W, et al. Controlling factors of coalbed methane occurrence below redbeds in Xutuan mine: Caprock thickness below redbeds [J]. Journal of Natural Gas Science and Engineering, 2021, 96
[13] Li Wen. The occurrence pattern and main controlling factors of coalbed methane in the Aihai mining area [J]. Coal Technology, 2023, 42 (11): 157-161.
[14] Dan Chuan, Zhang Yaya, Zou Yunlong, et al. Multivariate data fusion analysis of gas content and determination of outburst critical values [J]. Energy and Environmental Protection, 2023, 45 (04): 16-20.
[15] AQ 1018-2006, Prediction Method for Mine Gas Emission [S].